Scientific Research Publishing

Open Journal of Geology, 2024, 14, 746-759
https://www.scirp.org/journal/ojg
ISSN Online: 2161-7589
ISSN Print: 2161-7570

Comparative Study between Dielectric Properties and Compaction Parameters: Case Study on Three Laterite Quarries

Cheikh Diallo Diene[1,2*], Sabou Sarr[1], Abdoulaye Cissé[1], Mapathé Ndiaye[1,2]

[1]Laboratoire de Géophysique, UFR Sciences de l'Ingénieur, University Iba Der Thiam, Thies, Senegal
[2]Laboratoire de Modélisation et de Mécanique des Sols, UFR Sciences de l'Ingénieur, University Iba Der Thiam, Thies, Senegal
Email: *cheikhdiallo.diene@univ-thies.sn

How to cite this paper: Diene, C.D., Sarr, S., Cissé, A. and Ndiaye, M. (2024) Comparative Study between Dielectric Properties and Compaction Parameters: Case Study on Three Laterite Quarries. *Open Journal of Geology*, **14**, 746-759.
https://doi.org/10.4236/ojg.2024.148032

Received: July 18, 2024
Accepted: August 10, 2024
Published: August 13, 2024

Abstract

This work studies the variability of the relationship between relative permittivity and compaction parameters as a function of certain geotechnical properties for different laterite types. This study allows to purpose the dielectric permittivity as a third compaction parameter allowing to obtain a non destructive control méthod. Preliminary studies on Diack laterite had shown a good correlation. Additional investigations are carried out to verify the possibility of generalizing this correlation to three new laterite careers: Ngoudiane, Yéba and Fandene. To proceed, particle size analysis, Atterberg limits, specific weight tests and compaction according to the modified Proctor test were performed on laterite samples. Using the radar method, experimental permittivities are determined for laterite samples by the point method of propagation times and confirmed by the diffraction hyperbole method. The geotechnical and radar data obtained allowed correlations between permittivity and water content on the one hand and between permittivity and dry density on the other. The results show that the maximum dry density as a function of permittivity corresponds with the optimum Proctor, which confirms the results previously obtained on Diack laterite.

Keywords

Radar, Laterite, Moisture Content, Dry Density, Permittivity, Geotechnical Properties

1. Introduction

Nowadays, we are witnessing more and more the premature degradation of the pavements raising questions about the quality of the materials used and their

modes of execution. One of the most popular materials in Senegal is laterite, which is characterized by high heterogeneity, variability in texture and grain size, sometimes in the same deposit [1]. This variability makes it difficult to strictly control in situ compaction by conventional processes.

Ndiaye *et al.* 2023 [2], suggested a control of in situ compaction of laterites by radar method by proposing a relative permittivity relationship—water content and relative permittivity—dry density. This relationship seeks to identify the optimal compaction parameters from an optimal permittivity. This approach was to allow indirect control of the compaction quality by the Ground Penetrating Radar (GPR) method [2].

Indirect method control of compaction not only saves time but is also a non-destructive means of quality control over large areas of compaction quality. In order to study the domain of validity of the permittivity relationship and compaction parameters in the case of laterites that constitute heterogeneous materials, we will study three additional laterite samples in order to be built on the effect of geotechnical parameter variability. Thus, we will proceed to a parametric study from different types of laterites.

Several relationships developed in the literature establishing a relationship between for example the water content by volume and the permittivity as the case of the formula of Topp [3] and the relation of CRIM [4] which are valid only for soils of uniform granulometry, which is not the case for most laterites.

The objective of this work is to study, from additional laterite data, the usability of dielectric permittivity in the quality control of laterite compaction. In other words, this study will make it possible to establish the variability in the determination of the optimum proctor during a situ control from the permittivity values determined by radar method.

2. Material and Method

This work combines an experimental study on samples with a numerical simulation to anticipate the nature of the expected results. The steps in our process can be summarized as follows:

- Step 1: conducting laboratory geotechnical tests;
- Step 2: Dielectric characterization of samples by radar method;
- Numerical simulation of the radar response on samples investigate to confirm results and facilitate interpretation.

The laterite samples used in this study come from three quarries in the Thiès region of Senegal: the quarry of Fandène, Yéba and Ngoundiane. Laterites were characterized in the laboratory by particle size analysis [5], Atterberg limits [6], specific weight [7] before compaction according to the modified Proctor test [8].

Laterite permittivities were determined in the laboratory by radar method. In the radar method, an electromagnetic pulse is sent into the structure examined via a transmitting antenna at a determined central frequency. This impulse is propagated by attenuating in the materials. At each interface of different dielectric properties, part of the energy is reflected back to the surface and recorded by

the receiving antenna. The result is a profile or radargram [9] represented with a color scale correlated to the amplitudes of the signals and giving geometric information on the auscultated structure.

The propagation of radar waves in a field is governed by the Maxwell equations [10]. The average speed of propagation of radar waves in a geological environment is written:

$$v = \frac{3 \times 10^8}{\sqrt{\varepsilon_r}} \quad (1)$$

where ε_r is the relative permittivity of the medium.

The dielectric permittivity of a material reflects its ability to be polarized under the influence of an electric field, which causes the relative displacement of positive and negative related charges [11].

The radar measuring device used is the GSSI Structure Scan comprising a SIR 3000 acquisition unit [12] connected to a 1.6 GHz center frequency GSSI antenna mounted on a 619 trolley.

The equipment also includes a measuring table with a circular opening allowing the trolley to contact the CBR mould (**Figure 1**).

Figure 1. Acquisition of radar data on laterite samples.

Dielectric permittivity is determined using two methods:

- **Arrival Time Point Method** [13] which consists of locating the t1 time corresponding to the air-ground interface and the t2 time corresponding to the material interface—spacer disk.
- **Diffraction hyperbole method** [14] which consists in creating a detectable contrast between the interfaces of the materials; which is materialized by the appearance of diffraction hyperboles whose outer curvature corresponds to the velocity of the upper layer which increases with the radius of curvature [15]. To do this, we have, during the Proctor test, intercalated the mold, 5.5 cm from the surface, a cylindrical tube 6 cm long and 2 cm in diameter (**Figure 2**). The tube and arranged in the axis of the release screws so that the passage of the trolley is made perpendicular to the metal tube (**Figure 2**).

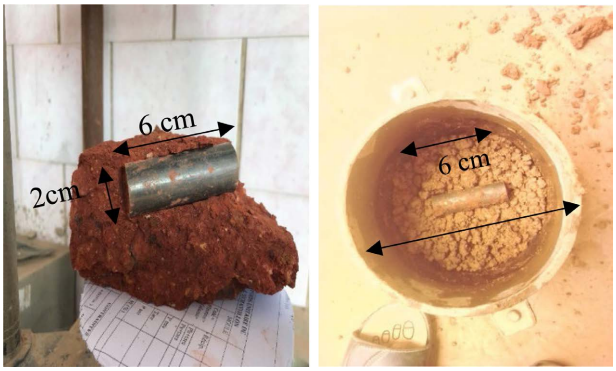

Figure 2. Proctor test with cylindrical bar.

In order to facilitate the identification of facies present in the radargram, we performed a numerical simulation of the propagation of radar waves in a Proctor mold containing materials under different conditions. The different scenarios were simulated using GprMax 2D software [16] (**Table 1**).

Table 1. Simulated scenarios.

Scenario	Material
1	Cylindrical mold + dry laterit
2	Cylindrical mold + saturated laterit
3	Cylindrical mold + dry laterit + inclusion metal cylinder at mid-height
4	Cylindrical mold + saturated laterit + inclusion metal cylinder at mid-height

For the different modeling scenarios, we considered a cylindrical modified Proctor mold with diameter 15.7 cm and height 12.6 cm. The mold is filled with dry laterite of properties: $\omega = 8\%$, $\varepsilon_s = 3$, $\mu_r = 1$, $\sigma = 0.001$. In the case of saturated laterite, the properties considered are $\omega = 31\%$, $\varepsilon_s = 30$, $\mu_r = 1$ H/m, $\sigma = 0.1$S/m. (ω is moisture content, μ_r is magnetic permeability, σ represents the electrical conductivity).

In laterite sample, an inclusion of cylindrical metal tube of length 7 cm and diameters 3 cm allows to generate a hyperbola used in the determination of permittivity.

The model geometry and radar signal simulation parameters are shown in the following table (**Table 2**):

Table 2. Model geometry and radar signal simulation parameters.

$\Delta x = \Delta y = \Delta l$ (mm)	2
Δt (ns)	2.364×10^{-9}
Iteration numbers	120
Emetter position (x, y) (m)	(0.04; 0)
Receiver position (x, y) (m)	(0.05; 0)
Frequency of antenna (MHz)	1600

Simulations were performed for each model with the generation of 120 radar tracks or A-Scan [17]. The 120 A-scans were compiled to generate a B-Scan [18].

3. Results and Discussions

3.1. Geotechnical Characterization

The results of the specific weight test are shown in Table 3.

The results of the Atterberg Limits test are shown in Table 4.

The results of the particle size analysis [16] are shown in Figure 3.

Table 3. Specific weight test.

Weight Pycnometer N°	Yéba		Ngoundiane	Fandene
	A	B	A	B
Pycnometer: P1	109.28	123.18	100.06	123.06
Pycnometer + material: P2	159.28	173.18	150.06	173.06
Pycnometer + material + eau P3	388.4	401.84	380.83	400.39
Pycnometer + water: P4	958.55	371.84	348.65	371.74
Specific weight	2.49		2.81	2.34

Table 4. Summary of atterberg boundary results.

	Liquidity limit (WL)	Plasticity limit (WP)	Plasticity Index (IP)
Ngoundiane	42.4	21.85	20.7
Yéba	42.5	14	28.8
Fandene	44.8	23.86	20.9

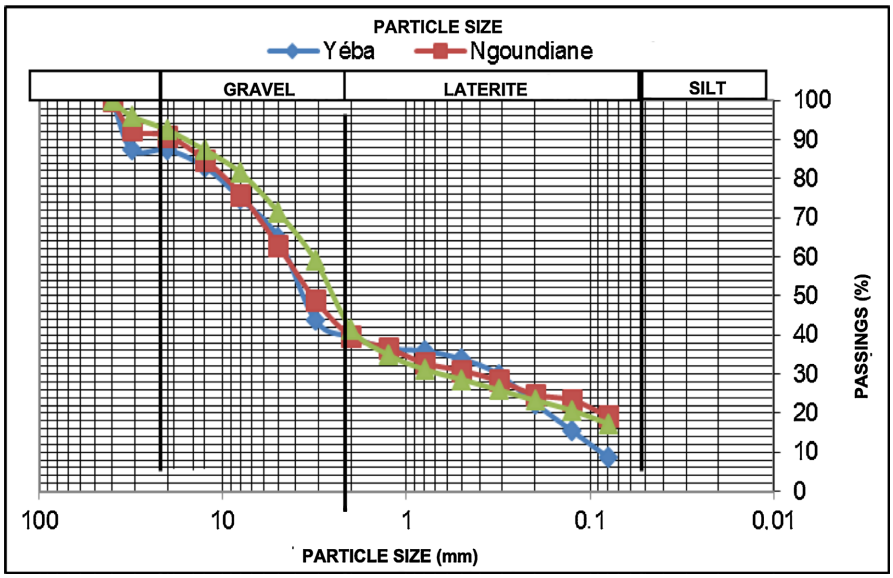

Figure 3. Particle size distribution of the three laterites.

The results of the Proctor trial are shown in Figure 4.

For each dry density, and specific density, the porosities ϕ were determined (Table 5).

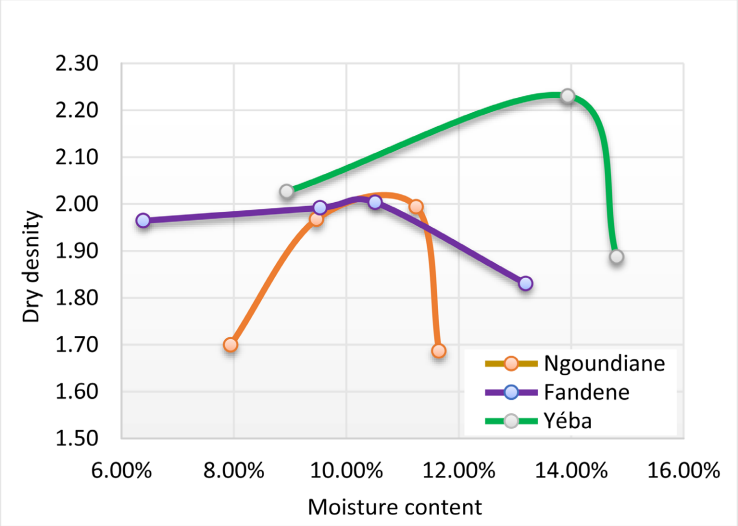

Figure 4. Proctor curves of the three laterite samples.

Table 5. Porosities of different laterites.

Site	ρ_d	ρ_s	ϕ	ϕ_{moy}
Yéba	2.09	2.49	0.16	0.15
	2.14		0.14	
	2.08		0.16	
Ngoundiane	1.7	2.34	0.27	0.22
	1.97		0.16	
	1.99		0.15	
	1.69		0.28	
Fandene	2.09	2.34	0.11	0.11
	2.14		0.09	
	2.08		0.11	
	2.08		0.11	

3.2. Results of Simulations under GPRrmax

The no-inclusion scenario (Figure 5) was performed to show the influence of edge effects. At the end of the simulation, the profile obtained shows that the edge effect is not significant in the results of the appearance of reflections.

The air being a homogeneous isotropic medium, when a radar wave propagates in the latter, it encounters no change in the dielectric parameters (Figure 6). The homogeneity of this medium causes the wave to propagate without reflection to the air/laterite interface.

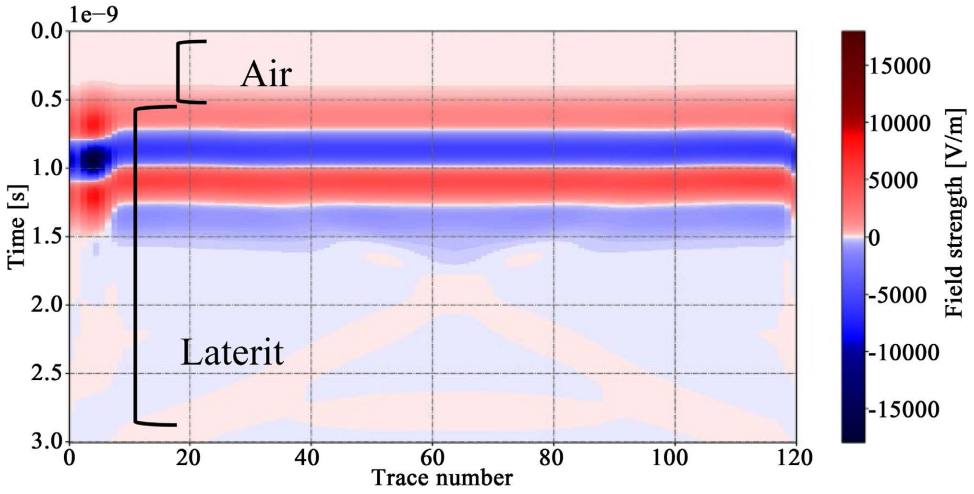

Figure 5. Scenario 1: Without metal inclusion.

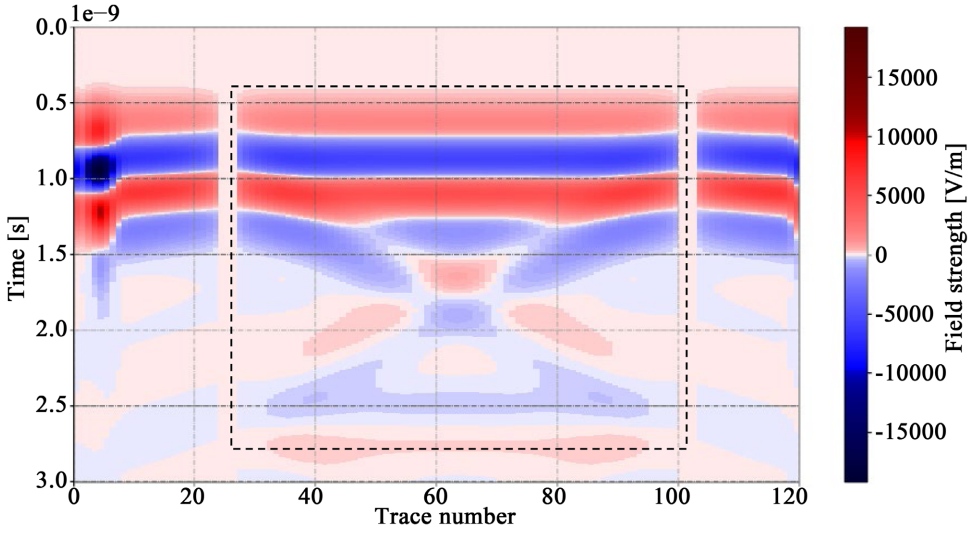

Figure 6. Scenario 2: Saturated laterite without metal inclusion.

The appearance of the first positive reflections marks the penetration of the wave into the material from the air/laterite interface. In this model, the walls of the mold are well identified and that inside soft reflections are noted showing a material without major contrast.

In this dry soil model with inclusion (**Figure 7**), we note the appearance of a diffraction hyperbole corresponding to the radar signature.

Scenario of **Figure 8** shows that at the wet laterite/metal inclusion interface, the radar wave is reflected by forming a diffraction hyperbole. The shape of the hyperbola is more pronounced than in the case of dry laterite. To this is added the presence of the two outer edges of the Proctor mold which are visible only in the case of saturated laterite. Indeed, the high reflection amplitudes in saturated laterite contrast with the amplitudes in total reflection observed at the walls of the mold.

The speed of the radar wave in wet laterite is low because the relative permit-

tivity is high. The decrease in speed is due to the attenuating effect of water in saturated laterite.

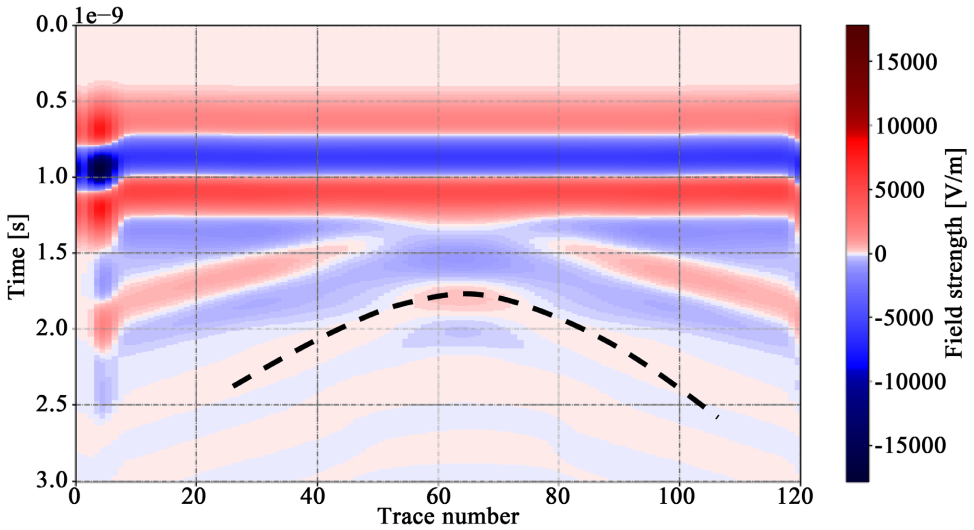

Figure 7. Scenario 3: Dry laterite with metal inclusion.

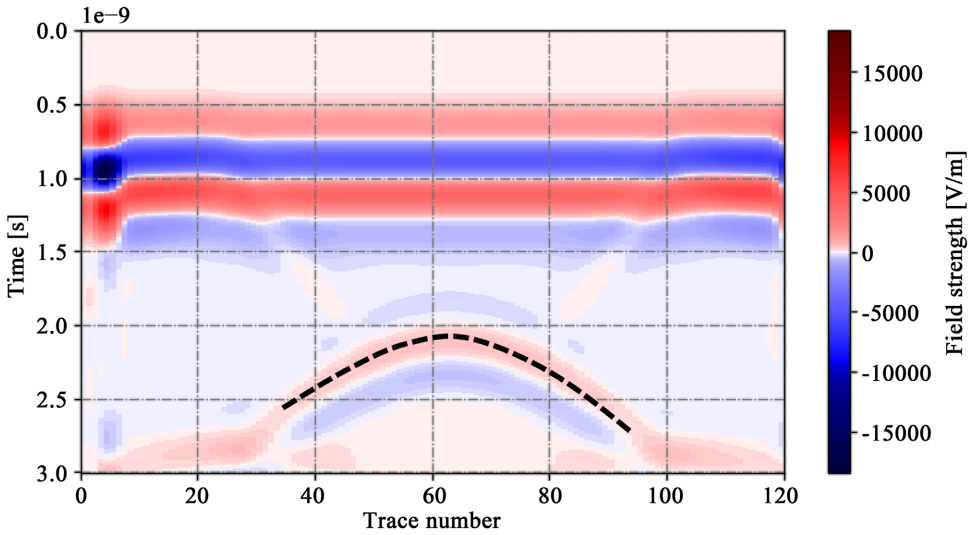

Figure 8. Scenario 4: saturated laterite with metal inclusion.

3.3. Results of Experimental Radar Measurements

The results of the three radar profiles obtained on mussels with optimal water content are presented in Figures 9-11.

In order to better exploit and synthesize the results, the data obtained with the modified Proctor test and the permittivities obtained by radar method are summarized in Table 6.

The difference between the permittivities obtained by the arrival time point method and those with the diffraction hyperbole method can be explained by the fact that in some cases, the hyperboles were not clear on the profile (Figure 11). This may be due to a risk of slight displacement of the cylindrical tube during

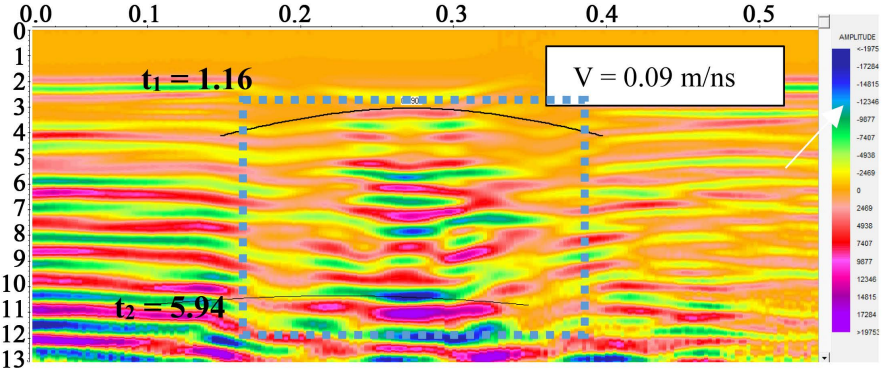

Figure 9. Radargram obtained at the optimal water content on the laterite of the Yeba site.

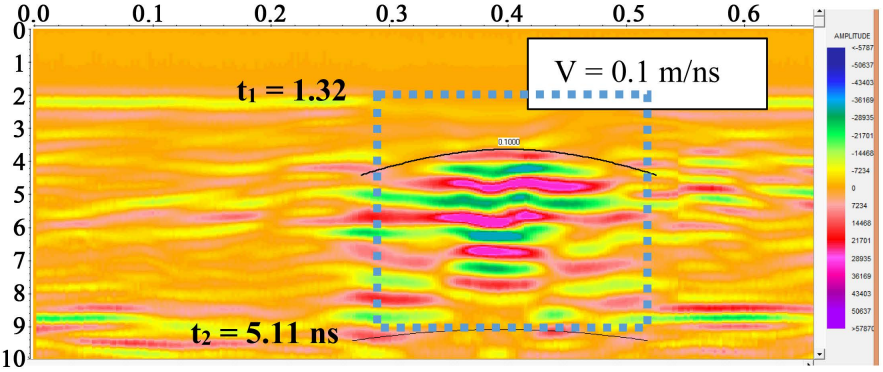

Figure 10. Radargram obtained at the optimal water content on the laterite of the Ngoundiane site.

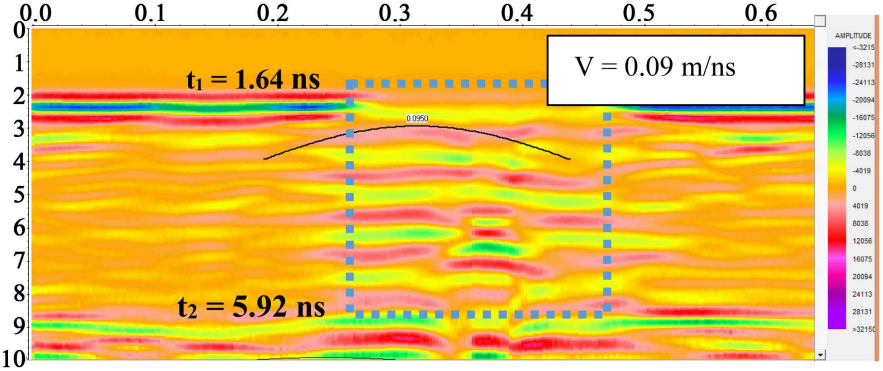

Figure 11. Radargram obtained at the optimal water content on the laterite of the Fandene site.

compaction. Therefore, the values found with the arrival time point method are assumed to be more reliable.

To study the permittivity/water content/dry density relationship, we superimposed the radar data and the compaction data.

We find that for water content values between 8% and 9.5%, the dry density increases considerably while the permittivity is almost static.

Indeed, Ngoundiane laterite has significant porosity values, which makes

Table 6. Summary of permittivities calculation results.

Sites \ Parameters	$\omega(\%)$	ρ_d (g/cm³)	ε_r (point)	ε_r (hyperbola)
Yéba	8.94%	2.09	8.95	12.46
	13.95%	2.14	12.78	14.06
	14.81%	2.08	9.09	11.11
Fandene	6.39%	1.96	7.47	6.81
	9.54%	1.99	10.78	9.97
	10.51%	2	11.36	11.11
	13.19%	1.83	10.17	9.97
Ngoundiane	7.94%	1.7	9.00	9.72
	9.47%	1. 97	11.11	9.92
	11.14%	1.99	12.46	11.73
	11.65%	1.69	9.00	8.72

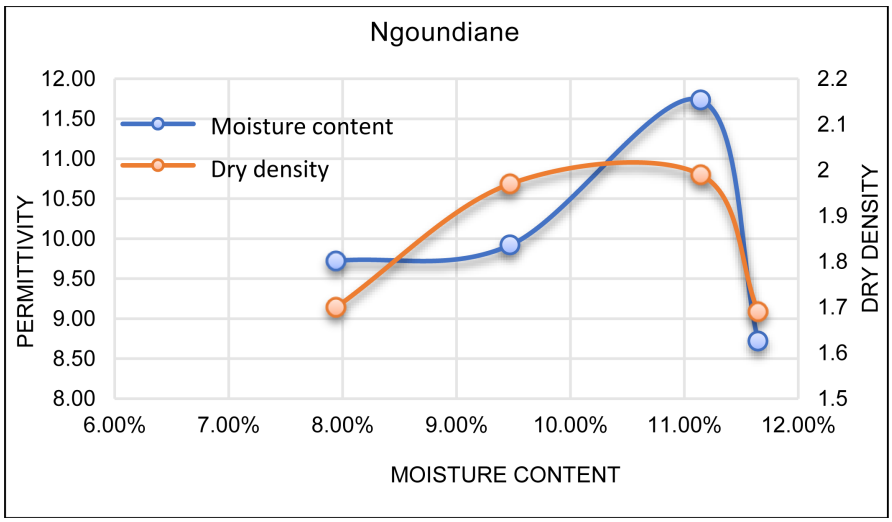

Figure 12. Relationship moisture content-permittivity-dry density of Ngoundiane laterite.

compaction easily increases dry density; but since there is a large volume of air with low water content, the permittivity always keeps low values close to the air permittivity. And when the water content becomes important, the air is expelled and replaced by water, which leads to a notorious evolution of permittivity.

On the other hand, in the wet branch there is a sharp drop in permittivity and dry density. Indeed, in addition to the action of the attenuation of the radar signal, we have assumed a possible return of the air since this very porous material remains under saturated, and that overcompaction has the effect of destabilizing the tightening.

While the dry density evolves very slowly in the dry branch due to a low porosity of this material, the permittivity increases considerably until optimum

since the sample does not contain much air.

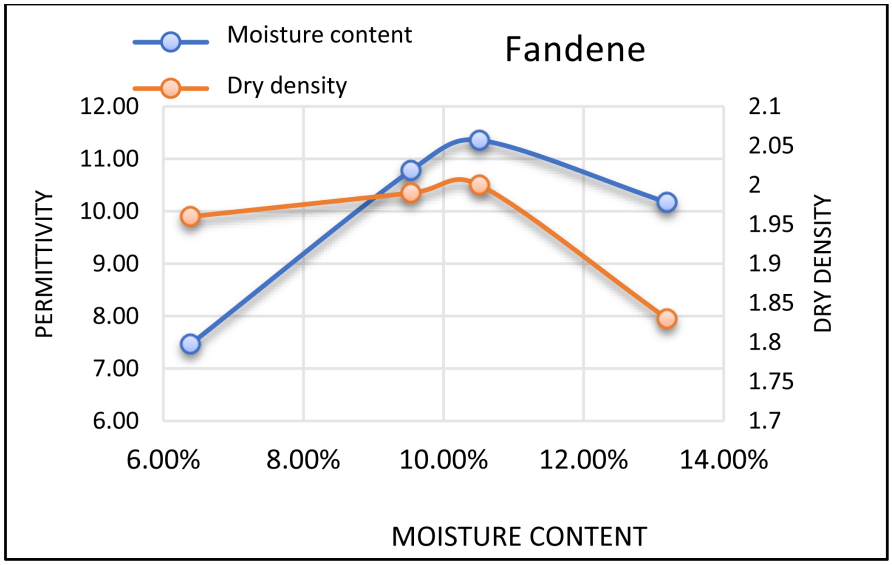

Figure 13. Relationship moisture content—permittivity-dry density of Fandene laterite.

Indeed, when the porosity of the material is low and the water content is not negligible, then the volume of air is very limited, which means that compaction has a lesser effect on material density while permittivity can change rapidly since the material has good moisture.

Beyond the optimum Proctor, dry density and permittivity are experiencing the same decline. This decrease in permittivity is due to the attenuation of the radar signal.

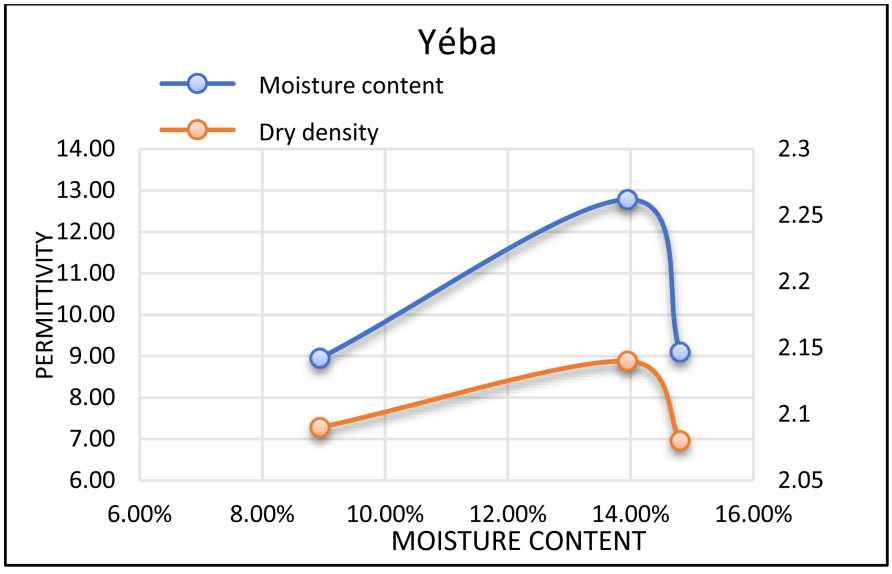

Figure 14. Relationship moisture content—permittivity-dry density of Yeba laterite.

We find that the permittivity increases with the same rate as the dry density in the wet branch and reaches its peak at the optimum Proctor.

This can be explained by the increase in water content but also by the decrease of the air fraction in the material due to compaction, both contributing to increase the relative permittivity of the material.

In the wet branch, there is an instantaneous decrease in dry density and permittivity due to the fact that at the optimum point, the soil with its very high clay content has reached its plastic limit (WL = 14%). Given that the radar signal is difficult to propagate in clays and the limited plasticity, the possibility for free water to polarize to create currents of displacement, hence the reasons for this decrease.

In synthesis, in the dry branch, we have a simultaneous increase in dry density and permittivity (**Figures 12-14**). This is due to the fact that in this part, the volume of the voids is much larger, so the compaction helps to tighten the grains together resulting in an increase in dry density. At the same time, the reduction of the air volume associated with the gradual increase of the water content leads to an increase of the relative permittivity until the Proctor optimum.

Beyond the optimum, there is a decrease in dry density and permittivity.

This drop in permittivity can be explained by the fact that the water content is very high in this part; which promotes a strong presence of conduction currents, so we tend to obtain a strong attenuation of the signal; which is verifiable on some high water content radargrams by a progressive loss of signal (**Figure 9**).

Given that $\alpha = 1.69\frac{\sigma_e}{\sqrt{\varepsilon_r}}$, an increase in water content results in an increase in conductivity which results in an increase in the attenuation of the radar signal. This results in a decrease in permittivity.

The general appearance of permittivity increases and decreases with compaction, however each type of laterite may have small variations of the general appearance depending on its geotechnical properties

In summary, the overlap between laterites of the three quarries shows that:

- The increase in permittivity is a function of the increase in water content, porosity but also dry density (**Figure 9**).
- The homogeneous character contributes to the decrease of the permittivity because when there are less granular classes, the material is less polarizable. This is the case of Ngoundiane laterite
- The strong presence of coarse particles has an effect on the slow evolution of relative permittivity because it favors the presence of air. This is the case of Fandene laterite.
- A strong presence of fine particles corresponding to clay particles has an effect on the increase of permittivity since clay has higher permittivity values than other minerals (**Table 1**). This is the case of Yeba's laterite.

It also appears that the more the plasticity index Ip of the soil increases the more permittivity increases. Indeed, soils that have important plasticity domains are soils that have the ability to absorb a large amount of water without a large modification, so their polarizability is limited; which makes them have a lower permittivity.

Since the maximum dry density coincides with the maximum permittivity for all laterites tested, it is possible to predict the maximum dry density value of these laterites from a radar test. These results may also allow us to have a third compaction parameter in the technical specifications.

4. Conclusions

This study allowed to study the variability of the relationship between relative permittivity and compaction parameters as a function of geotechnical properties and to establish the conditions and limits of the use of dielectric permittivity in quality of laterite compaction.

The permittivities of the compacted laterites were determined from a radar test using waves whose nature of propagation was determined after a simulation on a mold under different conditions. The analysis of permittivity results from the specific geotechnical characteristics of each laterite led to the following conclusions:

- the coarse-grained laterites have more limited permittivity values.
- Laterits with a higher plasticity index have higher permittivities.
- Proctor test results superimposed on permittivity results showed that permittivity increases proportionally with water content to the maximum density point from which it decreases inversely.
- For high porosity laterites, dry density changes faster than permittivity, unlike low porosity laterites where permittivity changes faster than dry density. In short, the variation of permittivity depended not only on water content and dry density but also on certain geotechnical properties such as granulometry, porosity and plasticity index.

These results predict the maximum dry density and optimum water content of laterite from a radar test and thus add permittivity as a third control parameter—laterite layer quality.

It would be interesting to test this study on other materials such as cement soils, sands or clays. It would also be possible to confirm these results on an already compacted laterite layer.

Conflicts of Interest

The authors declare no conflicts of interest regarding the publication of this paper.

References

[1] Massamba, N. (2013) Contribution à l'étude de sols latéritiques du Sénégal et du Brésil. Doctoral Dissertation, Université Paris-Est et Université Cheikh Anta Diop (Dakar).

[2] Ndiaye, M., Ba, M., Kiendrebeogo, T. and Foudjo, L.E.G. (2023) Relative Dielectric Permittivity Variations during Compaction as a Mean of Compaction Quality Control: Case Study on Laterite Samples from Senegal. *International Journal of Geosciences*, **14**, 238-250. https://doi.org/10.4236/ijg.2023.142012

[3] Ground Penetrating, R. (2009) Ground Penetrating Radar: Theory and Applications.

[4] Vincent, G. (2019) Lois d'homogénéisation en électromagnétisme pour l'estimation de la teneur en eau des bétons. *Academic Journal of Civil Engineering*, **37**, 410-418.

[5] Jerˆome, F., *et al.* (2012) Analyses granulométriques. Principes et méthodes.

[6] Norme, N.F. (1993) Reconnaissance et essai de détermination des limites d'Atterberg.

[7] Norme, A. (1991) Détermination de la masse volumique de particules solides des sols. Méthode du pycnomètre à eau.

[8] Robert, M. and Delorme, J.-L. (2010) Comparaison des essais Proctor selon la norme NF et selon la norme EN.

[9] Belkadid, J., Bennani, S.D. and Rifi, M. (2006) Amélioration de la sensibilité de détection et de la qualité du radargramme d'un radar pénétrant GPR par une modulation micro-onde. *Annals of Telecommunications*, **61**, 565-577. https://doi.org/10.1007/bf03219923

[10] Huray, P.G. (2009) Maxwell's Equations. Wiley.

[11] Messaouda, K., Bouzar, S. and Brahmi, G. (2021) Caractérisation d'un sous-sol par méthode géoradar (GPR), Application pour le cas de la ville d'Alger.

[12] Juho, R. (2012) SIR-3000-maatutkan soveltuvuus teräsbetonirakenteiden tutkimiseen.

[13] Xavier, D., *et al.* (2001) Performances de radars d'auscultation des chaussées sur des sites tests. *Bulletin-Laboratoires des Ponts et Chaussees*, **2001**, 15-22.

[14] Yuan, H., Montazeri, M., Looms, M.C. and Nielsen, L. (2019) Diffraction Imaging of Ground-Penetrating Radar Data. *Geophysics*, **84**, H1-H12. https://doi.org/10.1190/geo2018-0269.1

[15] Mevel, J. (1976) Procédure de reconnaissance des formes a l'aide d'un radar monostatique. *Annales Des Télécommunications*, **31**, 111-118. https://doi.org/10.1007/bf02997593

[16] Giannopoulos, A. (2005) Modelling Ground Penetrating Radar by Gprmax. *Construction and Building Materials*, **19**, 755-762. https://doi.org/10.1016/j.conbuildmat.2005.06.007

[17] Yigit, E., Sabanci, K., Toktas, A., Ustun, D. and Duysak, H. (2018). Grain Moisture Detection by Using A-Scan Radar Measurement. 2018 *XXIIIrd International Seminar/Workshop on Direct and Inverse Problems of Electromagnetic and Acoustic Wave Theory*, Tbilisi, 24-27 September 2018, 222-224. https://doi.org/10.1109/diped.2018.8543311

[18] Özdemir, C., Demirci, Ş., Yiğit, E. and Yilmaz, B. (2014) A Review on Migration Methods in B-Scan Ground Penetrating Radar Imaging. *Mathematical Problems in Engineering*, **2014**, 1-16. https://doi.org/10.1155/2014/280738